# Dissipative Spin-Wave Diode and Nonreciprocal Magnonic Amplifier

Ji Zou,* Stefano Bosco, Even Thingstad, Jelena Klinovaja, and Daniel Loss
*Department of Physics, University of Basel, Klingelbergstrasse 82, 4056 Basel, Switzerland*

(Received 28 June 2023; accepted 1 December 2023; published 16 January 2024)

We propose an experimentally feasible dissipative spin-wave diode comprising two magnetic layers coupled via a nonmagnetic spacer. We theoretically demonstrate that the spacer mediates not only coherent interactions but also dissipative coupling. Interestingly, an appropriately engineered dissipation engenders a nonreciprocal device response, facilitating the realization of a spin-wave diode. This diode permits wave propagation in one direction alone, given that the coherent Dzyaloshinskii-Moriya (DM) interaction is balanced with the dissipative coupling. The polarity of the diode is determined by the sign of the DM interaction. Furthermore, we show that when the magnetic layers undergo incoherent pumping, the device operates as a unidirectional spin-wave amplifier. The amplifier gain is augmented by cascading multiple magnetic bilayers. By extending our model to a one-dimensional ring structure, we establish a connection between the physics of spin-wave amplification and non-Hermitian topology. Our proposal opens up a new avenue for harnessing inherent dissipation in spintronic applications.

DOI: 10.1103/PhysRevLett.132.036701

*Introduction.*—A main theme of magnonics is the utilization of spin waves, or their quanta magnons, for information processing and transmission, to develop innovative computing and communication technologies [1–7]. The ability to directionally control information transmission is a cornerstone in both classical and quantum information processing systems [8–10]. This control is facilitated through the employment of essential components such as diodes. In magnonics, a spin-wave diode, which permits the unidirectional transmission of spin waves, holds critical importance. Such a device can function as a spin-wave rectifier and foster the development of more efficient and adaptable spintronic devices, such as memory devices, sensors, and spin-wave-based logic circuits. It stimulated numerous recent studies on nonreciprocal couplings and chiral spin waves, both theoretically [11–14] and experimentally [15–18]. Several proposals for spin-wave diodes have emerged [19–24], relying on anisotropic exchange, dipolar or Dzyaloshinskii-Moriya interactions (DMI). These proposals share one common feature—they build upon purely coherent interactions in the system, requiring low levels of damping for high diode efficiency.

In this Letter, we provide a different paradigm for realizing a spin-wave diode at low temperatures that leverages *dissipative* couplings in the system, which allows us to achieve a perfect spin-wave diode even when the damping is comparable to the coherence interactions [25]. We consider an experimentally feasible ferromagnetic bilayer structure separated by a nonmagnetic spacer layer as depicted in Fig. 1(a). We demonstrate that this spacer not only mediates coherent couplings such as the interlayer DMI but also gives rise to a dissipative coupling and local damping. Interestingly, we find that an ideal diode, facilitating unidirectional transmission while completely blocking the opposite direction, can be achieved in the presence of significant dissipative coupling at low temperatures compared to the magnon resonance frequency, when it is balanced with the DMI. We thus refer to such a system as a dissipative spin-wave diode.

We further demonstrate that when the magnetic layers are incoherently pumped, nonreciprocal amplification of spin waves can occur. In this scenario, the unidirectional

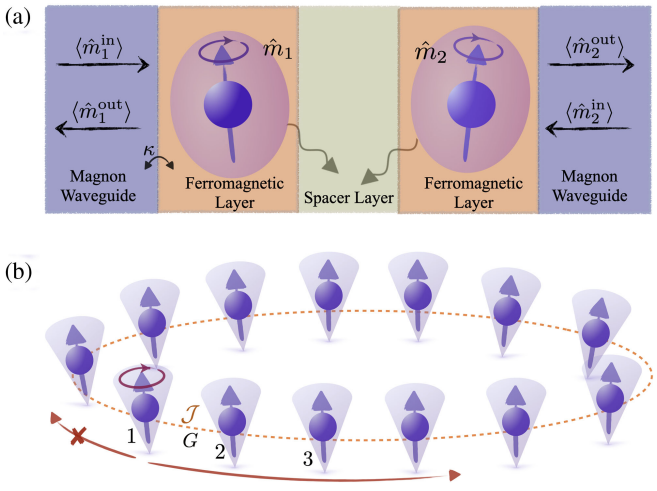


FIG. 1. (a) Schematic diagram of the *dissipative* spin-wave diode realized by a magnetic bilayer coupled through a nonmagnetic spacer. (b) Generalization to many magnetic layers coupled to their neighboring sites via both coherent and dissipative couplings, $\mathcal{J}$ and $G$. When these couplings are balanced, the launched spin wave in the system can only travel unidirectionally.

 

spin-wave signal is enhanced. This type of amplifier has the potential for broad applications in magnonics. It is capable of effectively filtering out thermal noise and also enables the detection of weak signals while simultaneously protecting them from unwanted backaction caused by the readout devices [26–29]. The gain of the amplifier can be enhanced through the cascading arrangement of several magnetic bilayers. We thus extend our study to an array of magnetic layers, where neighboring sites are coupled through both coherent and dissipative couplings. When these couplings are balanced, the spin waves launched in the system can only propagate unidirectionally, as depicted in Fig. 1(b). We further establish a connection between amplification and the non-Hermitian topology of the dissipative magnetic system [30–34].

*Model and mean-field dynamics.*—We model the magnetic bilayer system sketched in Fig. 1(a) with Hamiltonian

$$\hat{H} = \hat{H}_M + \hat{H}_E + \hat{H}_{ME}, \tag{1}$$

where $\hat{H}_M = -b(\hat{S}_1^z + \hat{S}_2^z)$ governs the dynamics of the two magnetic layers described by macroscopic spins $\hat{S}_i$ in an applied magnetic field $b\hat{z}$ whereas $\hat{H}_E$ stands for the Hamiltonian of the spacer. The coupling between the magnetic and spacer layers is captured by $\hat{H}_{ME} = \lambda \sum_{i=1,2}(\hat{S}_i^- \hat{E}_i^- + \text{H.c.})$, with $\hat{S}^{\pm} \equiv \hat{S}^x \pm i\hat{S}^y$ and coupling strength $\lambda$. Here $\hat{E}_i^{\pm}$ are operators representing degrees of freedom in the spacer layer. For the realization of such a heterostructure, one may use an insulating spacer such as doped gallium-gadolinium garnet, with the magnetic layer being yttrium iron garnet (YIG). In this case, $\hat{E}_i^{\pm}$ represents phonon fields [35–37]. We note that time-reversal symmetry is broken, allowing for the linear coupling in $\hat{H}_{ME}$ [38]. Another promising platform is to use a magnetic material like cobalt (Co) or a $Co_xFe_{1-x}$ alloy and employ a metal spacer such as iridium (Ir) or ruthenium (Ru). Here, the macroscopic spins couple to the spin of itinerant electrons. After performing the Holstein-Primakoff transformation [39] and keeping leading terms, we arrive at $\hat{H}_M \approx \hbar\Omega \sum_{i=1,2} \hat{m}_i^\dagger \hat{m}_i$ and $\hat{H}_{ME} = \sum_{i=1,2}(\hat{m}_i^\dagger \hat{E}_i^- + \text{H.c.})$. Here, $\hat{m}_i$, $i = 1, 2$ are magnon operators for two magnetic layers, obeying $[\hat{m}_i, \hat{m}_j^\dagger] = \delta_{ij}$. The ferromagnetic resonance frequency, denoted as $\Omega$ and typically residing within the gigahertz regime, is proportional to the applied magnetic field. We have absorbed constant prefactors into the definition of $\hat{E}_i^{\pm}$.

To examine the dynamics of the two magnetic layers, we trace out the spacer [40] and obtain the following master equation for the (reduced) density matrix $\hat{\rho}$ for two magnon modes at zero temperature [41]:

$$\frac{\mathrm{d}}{\mathrm{d}t}\hat{\rho} = -\frac{i}{\hbar}[\hat{H}_M + \hat{H}_C, \hat{\rho}] + \sum_{k,j=1,2} \mathcal{L}_{kj}^{\downarrow}\hat{\rho}, \tag{2}$$

where the spacer-mediated coherent interaction reads:

$$\hat{H}_C = \mathcal{J}\hat{m}_1^\dagger \hat{m}_2 + \mathcal{J}^* \hat{m}_2^\dagger \hat{m}_1, \quad \text{with} \quad \mathcal{J} = \frac{\mathcal{G}_{12}^R(\Omega) + \mathcal{G}_{12}^A(\Omega)}{2\hbar}. \tag{3}$$

Here, the retarded and advanced Green's functions follow their standard definitions [49], $G_{12}^{R,A}(t) = \mp i\Theta(\pm t)\langle[\hat{E}_1^-(t), \hat{E}_2^+]\rangle$ [41,50], and we use $\mathcal{G}(\omega) = \int d\tau\, e^{i\omega\tau} G(\tau)$. The coherent coupling $\mathcal{J}$ is complex valued in general. Its real part stands for the symmetric exchange between the two magnetic layers, while the imaginary component represents the DMI, which is nonvanishing only when the spatial inversion symmetry of the spacer is broken [41]. Above, we neglect the dipolar interaction, which would only renormalize the coherent coupling. We eventually have an effective coupling strength (typically on the scale of megahertz in experiments) [51–53], which can be balanced by the dissipative coupling we introduce below. Thus, the dipolar coupling will not change our conclusion.

The second term in the master equation (2) accounts for the nonunitary (dissipative) evolution of the magnetization due to the spacer layer, with the following Lindblad form: $\mathcal{L}_{kj}^{\downarrow}\hat{\rho} = \gamma_{kj}^{\downarrow}[\hat{m}_j\hat{\rho}\hat{m}_k^\dagger - \frac{1}{2}\{\hat{m}_k^\dagger\hat{m}_j, \hat{\rho}\}]$. The dissipative parameters are given by $\gamma_{kj}^{\downarrow} = i\mathcal{G}_{kj}^{>}(\Omega)/\hbar^2$, where $G_{kj}^{>}(t) \equiv -i\langle\hat{E}_k^-(t)\hat{E}_j^+\rangle$ is the greater Green's function [49]. Here $\gamma \equiv \gamma_{jj}^{\downarrow}$ is real valued by its definition [41] and represents the local magnon decay, leading to the Gilbert damping. It falls within the megahertz regime when the induced Gilbert damping is $10^{-2}$–$10^{-3}$. Further, $G \equiv \gamma_{21}^{\downarrow}$ represents nonlocal damping of magnons in the two magnetic layers, and we refer to it as the dissipative coupling [54]. This nonlocal damping can be comparable in magnitude to the local damping in experiments [55,56]. It is in principle also tunable, as it is governed by the response function in the spacer, similar to the coherent coupling. Such dissipative coupling is a key ingredient in recent proposals for non-Hermitian topological magnonic phases [31–34] and has also been investigated in cavity magnonic [57–59] and photonic [25,60,61] systems. Its real and imaginary components correspond to the dissipative symmetric and DM-like interactions, respectively. The latter emerges only when the inversion symmetry is broken [41]. In the absence of spin pumping, the system is in its natural thermodynamic equilibrium and the dissipative coupling is constrained by the local damping $|G| \leq \gamma$ [54], which ensures the complete positivity of the system dynamics. While we have assumed zero temperature for simplicity, a general discussion of finite temperature is provided in the Supplemental Material [41], where the dissipative coupling is reduced: $G \to (1 - e^{-\beta\hbar\Omega})G$. Therefore, as long as the temperature is not higher than the resonance frequency $\Omega$,

we still have a substantial dissipative coupling, and the presence of finite temperature does not alter our conclusion.

We stress that the master equation approach employed above relies on two crucial approximations [41,62]. The first Born approximation is justified when the frequency scales associated with the spacer-induced magnon dynamics are smaller than the resonance frequency (gigahertz). This requires the spacer-induced magnon damping rate and the interlayer coupling to be in the megahertz regime, which is typically the scale observed in experiments [51–53]. The Markov approximation applies when the environmental correlation time (lifetime of particles in the spacer) is shorter than the spacer-induced dynamics (which is microseconds if the induced dynamics is about megahertz). Note that the relaxation time of electron spin in metal is typically less than nanoseconds. For insulating spacers, the phonon lifetime usually varies from picoseconds to nanoseconds [63,64]. Another Markov approximation requirement is a frequency-independent coupling, justified by the large magnon frequency relative to magnon damping [65].

We obtain the mean-field dynamics of two magnetic layers from the master equation (2) by evaluating

$$\frac{\mathrm{d}}{\mathrm{d}t}\langle \hat{m}_i\rangle = -\frac{i}{\hbar}\langle[\hat{m}_i, \hat{H}_M + \hat{H}_C]\rangle + \mathrm{tr}\left[\hat{m}_i \sum_{k,j} \mathcal{L}^{\downarrow}_{kj}\hat{\rho}\right], \quad (4)$$

which yields $i\mathrm{d}\boldsymbol{\psi}/\mathrm{d}t = \mathcal{H}\boldsymbol{\psi}$ with $\boldsymbol{\psi} \equiv (\langle \hat{m}_1\rangle, \langle \hat{m}_2\rangle)^T$ and an *effective* non-Hermitian Hamiltonian [41]:

$$\mathcal{H} = \begin{bmatrix} \Omega - i\gamma/2 & \mathcal{J}/\hbar - iG^*/2 \\ \mathcal{J}^*/\hbar - iG/2 & \Omega - i\gamma/2 \end{bmatrix}. \quad (5)$$

The non-Hermitian character reflects the dissipative nature of the magnetic dynamics. Here, $\langle \hat{m}_i\rangle \equiv \mathrm{tr}[\hat{m}_i\hat{\rho}] \propto \langle \hat{S}^x_i\rangle + i\langle \hat{S}^y_i\rangle$ is the in-plane spin component. We note that the phase of the dissipative coupling $G$ can be gauged away and absorbed into the definition of the coherent coupling $\mathcal{J}$ [only the relative phase $\Phi \equiv \arg(\mathcal{J}/G^*)$ matters]. For this reason, we assume that $G$ is positive valued and $\mathcal{J} = e^{i\Phi}|\mathcal{J}|$, henceforth.

*Dissipative spin-wave diode.*—To investigate the unidirectional transmission of spin waves, we couple magnon waveguides to the bilayer system, as depicted in Fig. 1(a), with a coupling rate of $\kappa$. The response of the system is described by the Green's function [49]:

$$\hat{G}(\omega) = \frac{1}{\omega - \mathcal{H}}, \quad (6)$$

where we replace the local damping $\gamma$ with $\Gamma = \gamma + \kappa$ in the Hamiltonian (5) to account for the additional channel for magnon leakage provided by the magnon waveguide. The magnitudes of the off-diagonal elements of $\mathcal{H}$ are different when the DMI and the dissipative coupling are nonvanishing. This signals the emergence of a nonreciprocal phenomenon in the bilayer structure. Of particular interest is the scenario where $|\mathcal{H}_{12}| = 0$ but $|\mathcal{H}_{21}| > 0$. This is achieved when the following condition is fulfilled:

$$\mathcal{J}/\hbar = iG/2. \quad (7)$$

Here, the dissipative coupling $G$ is balanced with the coherent coupling $|\mathcal{J}|$, which is purely DMI ($\Phi = \pi/2$). The scattering matrix, related to the Green's function via $\hat{S}(\omega) = 1 - i\kappa\hat{G}(\omega)$ as dictated by the input-output theory [66–68], at resonance frequency reads:

$$\hat{S}(\Omega) = \begin{bmatrix} \frac{\gamma-\kappa}{\gamma+\kappa} & 0 \\ \frac{4\kappa G}{(\gamma+\kappa)^2} & \frac{\gamma-\kappa}{\gamma+\kappa} \end{bmatrix}. \quad (8)$$

It relates the incoming and outgoing waves as shown in Fig. 1(a), $\boldsymbol{\psi}^{\mathrm{out}} = \hat{S}(\omega)\boldsymbol{\psi}^{\mathrm{in}}$, with $\boldsymbol{\psi}^{\mathrm{in}} \equiv (\langle \hat{m}^{\mathrm{in}}_1\rangle, \langle \hat{m}^{\mathrm{in}}_2\rangle)^T$. The nonunitarity observed in this scattering matrix arises from dissipation, while its asymmetry leads to the nonreciprocal behavior. Here the input-output theory is justified as the magnon couples to the magnon waveguide linearly with a constant coupling strength around the magnon resonance frequency.

We observe that left-propagating spin waves are entirely blocked, with a vanishing transmission coefficient $|\hat{S}_{12}|^2 = 0$. In contrast, waves traveling in the opposite direction maintain a finite transmission coefficient, realizing a perfect diode. Note that there is no amplification as $|\hat{S}_{21}|^2 \leq 1$ without spin pumping. Reflected spin waves are generally observed, with $\hat{S}_{11} \neq 0$. However, when the two magnon-decay channels (the magnon waveguide and the spacer) are matched $\gamma = \kappa$, the reflection coefficient vanishes, and the transmission coefficient reaches its maximal value $|\hat{S}_{21}|^2 = (G/\gamma)^2$ (a perfect transmission of spin wave is achieved when $G = \gamma$).

While condition (7) enables an ideal dissipative spin-wave diode, it is worth noting that a well-performing diode, with $|\hat{S}_{21}|^2 \approx 1$ and $|\hat{S}_{12}|^2 \ll 1$, can be attained without requiring fine-tuning of the parameters. We depict the transmission coefficients for the two opposite directions as functions of the ratio of the two couplings $|\mathcal{J}|/\hbar G$ and the ratio of the two dampings $\kappa/\gamma$ in Figs. 2(a) and 2(b). We observe that a large transmission coefficient in one direction and a small one in the opposite direction can be obtained over a wide range of parameter values. Besides, a perfect unidirectional spin-wave blockade, transmitting sizable signals in the opposite direction, can be accomplished over a bandwidth set by local damping $\gamma$ (megahertz regime), as depicted in Fig. 2(d).

We emphasize that the directionality of the spin-wave diode is determined by the sign of the DMI, $\mathcal{D} = |\mathcal{J}|\sin\Phi$. Specifically, when $\Phi = \pi/2$, spin waves propagating from right to left are blocked, while opposite traveling waves are blocked when the sign of $\mathcal{D}$ is flipped; see Fig. 2(c).

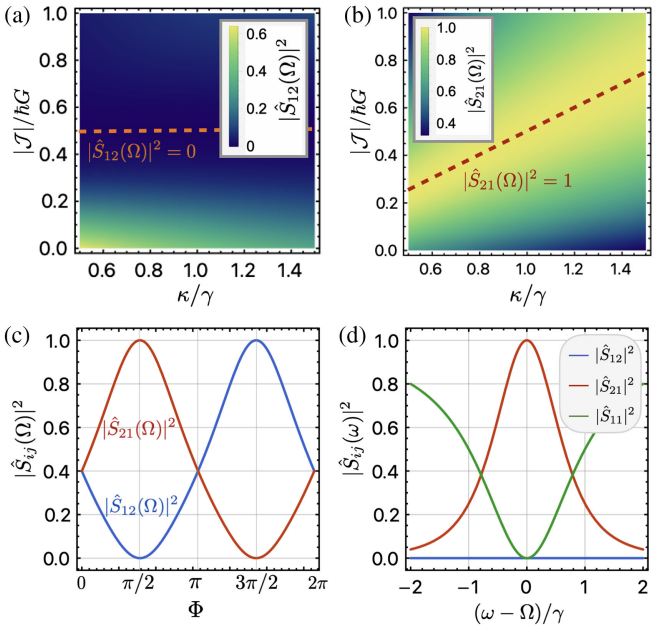


FIG. 2. Performance of a dissipative spin-wave diode. (a) The transmission coefficient $|\hat{S}_{12}(\Omega)|^2$ is plotted as a function of the coupling ratio $|\mathcal{J}|/\hbar G$ and the damping ratio $\kappa/\gamma$ with $\Phi = \pi/2$. An ideal diode is attained when the coherent and dissipative couplings are balanced (depicted by the dashed line), $|\mathcal{J}| = \hbar G/2$, independent of the ratio $\kappa/\gamma$. (b) The transmission coefficient $|\hat{S}_{21}(\Omega)|^2$ is shown as a function of $|\mathcal{J}|/\hbar G$ and $\kappa/\gamma$ with $\Phi = \pi/2$. The dashed red line indicates the condition for perfect transmission, $|\hat{S}_{21}(\Omega)|^2 = 1$, which is achieved when $\kappa = 2|\mathcal{J}|/\hbar$. (c) Transmission coefficients as a function of $\Phi$. At $\Phi = \pi/2, 3\pi/2$, where the coherent coupling is purely DMI, we observe a perfect dissipative diode. (d) Transmission and reflection coefficients as a function of spin-wave frequency with $\Phi = \pi/2$. In (c) and (d), we set $|\mathcal{J}|/\hbar = G/2$ and $\kappa = \gamma$. In all plots, we use $\gamma = G$ [41].

Pure DMI may be achieved in structures such as Co/Pt/Ir/Pt/Co, where it has been experimentally observed that both the DMI and the symmetric exchange coupling oscillate with the thickness of the spacer but have their peaks and valleys at different thicknesses [53]. This allows for the selection of certain thicknesses where the symmetric interaction is nearly zero, but the DMI remains substantial. One can further tune this interlayer DMI with symmetry-breaking fields, such as strain gradient [69–71], electric fields [72–75], or currents [76].

To measure the diode performance with finite symmetric coupling $J = |\mathcal{J}|\cos\Phi$, we introduce the diode efficiency:

$$\eta = \left| \frac{|\hat{S}_{12}|^2 - |\hat{S}_{21}|^2}{|\hat{S}_{12}|^2 + |\hat{S}_{21}|^2} \right|. \tag{9}$$

It is one when the system is a perfect diode (one direction is completely blocked). Assuming the DMI equals the dissipative coupling, we obtain the efficiency $\eta = 1/(r^2/2 + 1)$, where $r \equiv J/\mathcal{D} = \cot\Phi$ [41]. Note that this efficiency depends only on $\Phi$, independent of the incoming wave frequency and the local damping. Thus we can obtain a decent magnon diode, as long as $\mathcal{D} > J$.

We point out that the intrinsic Gilbert damping in the two magnetic layers, which we neglected, does not impact the diode efficiency [41]. It only reduces the unidirectional transmission amplitude since it provides another channel for magnons to decay. Sizable transmitted spin waves can be obtained with small damping magnets such as YIG or $Co_xFe_{1-x}$ [77].

*Unidirectional amplification of spin wave.*—Applying spin-transfer [78,79] or spin Seebeck [80] torques allows for the local pumping of magnetic layers out of their natural thermodynamic equilibrium. We leverage this to explore a broader range of experimentally tunable parameters. The spin pumping can be modeled as an additional term in Eq. (2) [81]: $\mathcal{L}^{\text{pump}}\hat{\rho} = \gamma^{\uparrow}\sum_{i=1,2}[\hat{m}_i^{\dagger}\hat{\rho}\hat{m}_i - \frac{1}{2}\{\hat{m}_i\hat{m}_i^{\dagger}, \hat{\rho}\}]$, with pumping rate $\gamma^{\uparrow} > 0$. This leads to a reduction of the local damping in the effective Hamiltonian (5) [41], where we now replace $\gamma$ with $\tilde{\gamma} \equiv \gamma - \gamma^{\uparrow}$. We point out that our system overall is still damped with effective damping parameter $\tilde{\gamma} > 0$.

To see how the pumping modifies the behavior of the spin-wave diode, we consider the scenario where the condition (7) is satisfied and the local damping is matched $\kappa = \tilde{\gamma}$ for simplicity. The scattering matrix for spin waves at resonance then reads:

$$\hat{S}(\Omega) = \frac{G}{\gamma - \gamma^{\uparrow}} \begin{bmatrix} 0 & 0 \\ 1 & 0 \end{bmatrix}. \tag{10}$$

We observe that spin pumping allows the realization of a unidirectional amplifier, where the spin-wave propagation is hindered in one direction, and the signal is enhanced in the opposite direction, when $G > \gamma - \gamma^{\uparrow}$. Note that the linear treatment breaks down when $G > 2\tilde{\gamma}$.

We emphasize that the unidirectional amplification is effective over a wide range of frequencies, as shown in Fig. 3. The dashed orange curve corresponds to the boundary that separates the parameter regimes with and without amplification, which is determined by $|\omega - \Omega| < \sqrt{\tilde{\gamma}(G - \tilde{\gamma})}$. Observably, the amplification bandwidth expands as the system undergoes pumping. At $\tilde{\gamma} = G/2$, the bandwidth is maximal $\sim G$ (megahertz regime).

*Cascading multiple magnetic layers.*—Employing a cascade of multiple magnetic bilayers can enhance the gain of the amplifier. Here we consider a ring structure for concreteness, as sketched in Fig. 1(b), where adjacent sites are coupled to each other via both coherent and dissipative coupling mediated by spacer layers between them. We describe the system with the following effective non-Hermitian Hamiltonian [82]:

$$\mathcal{H} = \sum_j \hbar(\Omega - i\gamma)\hat{m}_j^{\dagger}\hat{m}_j + \sum_j (\mathcal{J} - i\hbar G/2)\hat{m}_j^{\dagger}\hat{m}_{j+1} + \sum_j (\mathcal{J}^* - i\hbar G/2)\hat{m}_{j+1}^{\dagger}\hat{m}_j, \tag{11}$$

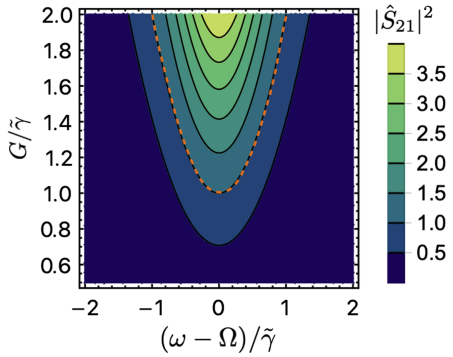


FIG. 3. Unidirectional amplification in the presence of spin pumping. The transmission coefficient $|\hat{S}_{21}|^2$ is shown as a function of frequency $\omega$ and the ratio of dissipative coupling $G$ to effective local damping $\tilde{\gamma}$. The dashed orange curve encloses the region with unidirectional amplification. We have assumed $\kappa = \tilde{\gamma}$ and condition (7) to get $\hat{S}_{12} = 0$.

which in momentum space takes the diagonal form $\mathcal{H} = \sum_k h(k)\hat{m}_k^\dagger \hat{m}_k$, where $h(k) = \hbar(\Omega - i\gamma) + (\mathcal{J} - i\hbar G/2)e^{ik} + (\mathcal{J}^* - i\hbar G/2)e^{-ik}$. The central quantity that governs the response of the system is the Green's function, which can be expressed as [41]

$$\langle l|\hat{G}(\omega)|j\rangle = \oint_{|z|=1} \frac{dz}{2\pi i} \frac{z^{l-j}}{z[\omega - h(z)/\hbar]}, \tag{12}$$

in real and frequency space. Here, $z = e^{ik}$ [83] and the integral can be evaluated by using Cauchy's residue theorem [84]. Considering again condition (7) to be satisfied, the second term in Hamiltonian (11) vanishes, indicating that magnons cannot travel clockwise. See Fig. 1(b). This is also reflected in the Green's function $\langle j|\hat{G}(\omega)|j+l\rangle = 0$, which vanishes for $l > 0$. On the other hand, we have $\langle j+l|\hat{G}(\omega)|j\rangle \sim \alpha^l$ for $l > 0$, where $\alpha = G/(\omega - \Omega - i\gamma)$ [41]. In the absence of spin pumping $G \leq \gamma$, the unidirectional spin wave in the system cannot be amplified for all frequencies since $|\alpha| \leq 1$.

When the system is pumped and $|\alpha| > 1$, the magnetic ring in Fig. 1(b) experiences an instability, where the spin wave keeps accumulating energy while circulating in the system, resulting in an unbounded growth of signal. The presence or absence of such amplification can be characterized through a topological index associated with the complex spectrum $h(k)$ [85]. Introducing a planar vector field $\mathbf{n}(k) = (-\mathrm{Im}h(k)/\hbar, \mathrm{Re}[\omega - h(k)/\hbar])$ [41] whose $x$ and $y$ components govern the dissipative and coherent dynamics of the system, respectively, the Green's function is $1/[n_y(k) + in_x(k)]$, which is nonanalytic at the origin $\mathbf{n}(k) = 0$. We therefore expect that whether $\mathbf{n}$ encloses the origin would lead to distinct physical phenomena. Indeed, the winding number, $2\pi\mathcal{N} \equiv \int_0^{2\pi} dk\, \hat{z} \cdot (\mathbf{n} \times \partial_k \mathbf{n})$, takes the value $\mathcal{N} = 0$ when $|\alpha| < 1$ and the spin wave decays, and $\mathcal{N} = 1$ when $|\alpha| > 1$ and the signal grows exponentially. The amplification of spin waves thus may serve as an experimental indicator of a topologically nontrivial magnonic phase [86].

*Conclusion.*—We investigated a magnetic bilayer system and showed that the spacer layer can mediate both coherent and dissipative couplings. When the resulting DM interaction is balanced with the dissipative coupling, we obtain a spin-wave diode. Furthermore, the spin-wave diode can be promoted to a unidirectional spin-wave amplifier by pumping. The gain can be improved by cascading several amplifiers. We also generalized our analysis to a one-dimensional ring structure and identify a connection between the physics of spin-wave amplification and non-Hermitian topology.

This work was supported by the Georg H. Endress Foundation and by the Swiss National Science Foundation, NCCR SPIN (Grant No. 51NF40-180604).

*ji.zou@unibas.ch

[1] A. V. Chumak, V. I. Vasyuchka, A. A. Serga, and B. Hillebrands, Magnon spintronics, Nat. Phys. **11**, 453 (2015).
[2] H. Yuan, Y. Cao, A. Kamra, R. A. Duine, and P. Yan, Quantum magnonics: When magnon spintronics meets quantum information science, Phys. Rep. **965**, 1 (2022).
[3] A. Chumak, P. Kabos, M. Wu, C. Abert, C. Adelmann, A. Adeyeye, J. Åkerman, F. Aliev, A. Anane, A. Awad *et al.*, Roadmap on spin-wave computing, IEEE Trans. Magn. **58**, 0800172 (2022).
[4] B. Lenk, H. Ulrichs, F. Garbs, and M. Münzenberg, The building blocks of magnonics, Phys. Rep. **507**, 107 (2011).
[5] A. Barman, G. Gubbiotti, S. Ladak, A. O. Adeyeye, M. Krawczyk, J. Gräfe, C. Adelmann, S. Cotofana, A. Naeemi, V. I. Vasyuchka *et al.*, The 2021 magnonics roadmap, J. Phys. Condens. Matter **33**, 413001 (2021).
[6] S. A. Nikitov, D. V. Kalyabin, I. V. Lisenkov, A. N. Slavin, Y. N. Barabanenkov, S. A. Osokin, A. V. Sadovnikov, E. N. Beginin, M. A. Morozova, Y. P. Sharaevsky *et al.*, Magnonics: A new research area in spintronics and spin wave electronics, Phys. Usp. **58**, 1002 (2015).
[7] H. Yu, J. Xiao, and H. Schultheiss, Magnetic texture based magnonics, Phys. Rep. **905**, 1 (2021).
[8] M. Tooley, *Electronic Circuits: Fundamentals and Applications* (Routledge, London, 2019).
[9] D. Crecraft and S. Gergely, *Analog Electronics: Circuits, Systems and Signal Processing* (Elsevier, New York, 2002).
[10] M. Rymarz, S. Bosco, A. Ciani, and D. P. DiVincenzo, Hardware-encoding grid states in a nonreciprocal superconducting circuit, Phys. Rev. X **11**, 011032 (2021).
[11] T. Yu, Y. M. Blanter, and G. E. W. Bauer, Chiral pumping of spin waves, Phys. Rev. Lett. **123**, 247202 (2019).
[12] T. Yu and G. E. W. Bauer, Efficient gating of magnons by proximity superconductors, Phys. Rev. Lett. **129**, 117201 (2022).

[13] H. Y. Yuan, R. Lavrijsen, and R. A. Duine, Unidirectional magnetic coupling induced by chiral interaction and nonlocal damping, Phys. Rev. B **107**, 024418 (2023).
[14] L. Udvardi and L. Szunyogh, Chiral asymmetry of the spin-wave spectra in ultrathin magnetic films, Phys. Rev. Lett. **102**, 207204 (2009).
[15] G. Gitgeatpong, Y. Zhao, P. Piyawongwatthana, Y. Qiu, L. W. Harriger, N. P. Butch, T. Sato, and K. Matan, Nonreciprocal magnons and symmetry-breaking in the noncentrosymmetric antiferromagnet, Phys. Rev. Lett. **119**, 047201 (2017).
[16] P. Wang, L. F. Zhou, S. W. Jiang, Z. Z. Luan, D. J. Shu, H. F. Ding, and D. Wu, Unidirectional spin-wave-propagation-induced seebeck voltage in a PEDOT:PSS/YIG bilayer, Phys. Rev. Lett. **120**, 047201 (2018).
[17] T. Yu, Z. Luo, and G. E. Bauer, Chirality as generalized spin–orbit interaction in spintronics, Phys. Rep. **1009**, 1 (2023).
[18] K. Di, V. L. Zhang, H. S. Lim, S. C. Ng, M. H. Kuok, J. Yu, J. Yoon, X. Qiu, and H. Yang, Direct observation of the Dzyaloshinskii-Moriya interaction in a Pt/Co/Ni film, Phys. Rev. Lett. **114**, 047201 (2015).
[19] K. A. van Hoogdalem and D. Loss, Rectification of spin currents in spin chains, Phys. Rev. B **84**, 024402 (2011).
[20] K. Nakata, P. Simon, and D. Loss, Spin currents and magnon dynamics in insulating magnets, J. Phys. D **50**, 114004 (2017).
[21] J. Lan, W. Yu, R. Wu, J. Xiao, Spin-wave diode, Phys. Rev. X **5**, 041049 (2015).
[22] K. Szulc, P. Graczyk, M. Mruczkiewicz, G. Gubbiotti, and M. Krawczyk, Spin-wave diode and circulator based on unidirectional coupling, Phys. Rev. Appl. **14**, 034063 (2020).
[23] M. Grassi, M. Geilen, D. Louis, M. Mohseni, T. Brächer, M. Hehn, D. Stoeffler, M. Bailleul, P. Pirro, and Y. Henry, Slow-wave-based nanomagnonic diode, Phys. Rev. Appl. **14**, 024047 (2020).
[24] S. Shichi, N. Kanazawa, K. Matsuda, S. Okajima, T. Hasegawa, T. Okada, T. Goto, H. Takagi, and M. Inoue, Spin wave isolator based on frequency displacement nonreciprocity in ferromagnetic bilayer, J. Appl. Phys. **117**, 17D125 (2015).
[25] A. Metelmann and A. A. Clerk, Nonreciprocal photon transmission and amplification via reservoir engineering, Phys. Rev. X **5**, 021025 (2015).
[26] T. Reichenbach and A. J. Hudspeth, Unidirectional mechanical amplification as a design principle for an active microphone, Phys. Rev. Lett. **106**, 158701 (2011).
[27] X. Wen, X. Zhu, A. Fan, W. Y. Tam, J. Zhu, H. W. Wu, F. Lemoult, M. Fink, and J. Li, Unidirectional amplification with acoustic non-Hermitian space-time varying metamaterial, Commun. Phys. **5**, 18 (2022).
[28] R. J. Doornenbal, A. Roldán-Molina, A. S. Nunez, and R. A. Duine, Spin-wave amplification and lasing driven by inhomogeneous spin-transfer torques, Phys. Rev. Lett. **122**, 037203 (2019).
[29] G. Petite, B. C. Johnson, W. K. H. Lange, and M. M. Salour, Observation of unidirectional amplified spontaneous emission induced by velocity-dependent light shifts, Phys. Rev. Lett. **45**, 1242 (1980).
[30] T. Yu, J. Zou, B. Zeng, J. Rao, and K. Xia, Non-Hermitian topological magnonics, arXiv:2306.04348.
[31] H. M. Hurst and B. Flebus, Non-Hermitian physics in magnetic systems, J. Appl. Phys. **132**, 220902 (2022).
[32] Y. Tserkovnyak, Exceptional points in dissipatively coupled spin dynamics, Phys. Rev. Res. **2**, 013031 (2020).
[33] B. Flebus, R. A. Duine, and H. M. Hurst, Non-Hermitian topology of one-dimensional spin-torque oscillator arrays, Phys. Rev. B **102**, 180408(R) (2020).
[34] K. Deng and B. Flebus, Non-Hermitian skin effect in magnetic systems, Phys. Rev. B **105**, L180406 (2022).
[35] S. Streib, H. Keshtgar, and G. E. W. Bauer, Damping of magnetization dynamics by phonon pumping, Phys. Rev. Lett. **121**, 027202 (2018).
[36] H. Y. Yuan, W. P. Sterk, A. Kamra, and R. A. Duine, Master equation approach to magnon relaxation and dephasing, Phys. Rev. B **106**, 224422 (2022).
[37] H. Y. Yuan, W. P. Sterk, A. Kamra, and R. A. Duine, Pure dephasing of magnonic quantum states, Phys. Rev. B **106**, L100403 (2022).
[38] G. Go, S. K. Kim, and K.-J. Lee, Topological magnon-phonon hybrid excitations in two-dimensional ferromagnets with tunable Chern numbers, Phys. Rev. Lett. **123**, 237207 (2019).
[39] T. Holstein and H. Primakoff, Field dependence of the intrinsic domain magnetization of a ferromagnet, Phys. Rev. **58**, 1098 (1940).
[40] H.-P. Breuer and F. Petruccione, *The Theory of Open Quantum Systems* (Oxford University Press, New York, 2007).
[41] See Supplemental Material at http://link.aps.org/supplemental/10.1103/PhysRevLett.132.036701 for (i) the master equation for the two magnetic layers at finite temperature, (ii) the non-Hermitian Hamiltonian for the mean-field dynamics, (iii) the scattering matrix for the spin-wave diode, (iv) discussion of the dependence of diode efficiency on symmetric exchange coupling and DMI, and (iv) the topological index and unidirectional amplification, which includes Refs. [42–48].
[42] P. Bruno and C. Chappert, Oscillatory coupling between ferromagnetic layers separated by a nonmagnetic metal spacer, Phys. Rev. Lett. **67**, 1602 (1991).
[43] Y.-J. Wu, Q.-Y. Xiong, H.-J. Duan, J.-Y. Ba, M.-X. Deng, and R.-Q. Wang, Interlayer RKKY interaction in ferromagnet/tilted Weyl semimetal/ferromagnet trilayer system, Phys. Rev. B **106**, 195130 (2022).
[44] J. Hermenau, M. Ternes, M. Steinbrecher, R. Wiesendanger, and J. Wiebe, Long spin-relaxation times in a transition-metal atom in direct contact to a metal substrate, Nano Lett. **18**, 1978 (2018).
[45] G. P. Srivastava, *The Physics of Phonons* (CRC Press, Boca Raton, 2022).
[46] K. Monikapani, V. Vijay, S. Harish, J. Archana, C. Muthamizhchelvan, and M. Navaneethan, Ultra-low thermal conductivity through the reduced phonon lifetime by microstructural and umklapp scattering in $Sn_{1-x}Mn_xSe$ nanostructures, J. Alloys Compd. **917**, 165152 (2022).
[47] C. Berk, M. Jaris, W. Yang, S. Dhuey, S. Cabrini, and H. Schmidt, Strongly coupled magnon–phonon dynamics in a single nanomagnet, Nat. Commun. **10**, 2652 (2019).

[48] L. Soumah, N. Beaulieu, L. Qassym, C. Carrétéro, E. Jacquet, R. Lebourgeois, J. Ben Youssef, P. Bortolotti, V. Cros, and A. Anane, Ultra-low damping insulating magnetic thin films get perpendicular, Nat. Commun. **9**, 3355 (2018).
[49] H. Bruus and K. Flensberg, *Many-Body Quantum Theory in Condensed Matter Physics* (Oxford University Press, New York, 2004).
[50] Here, $\langle \hat{A} \rangle$ stands for $\mathrm{tr}[\hat{\rho}_E \hat{A}]$, where $\hat{\rho}_E$ is the thermal state of the spacer.
[51] S. S. P. Parkin, N. More, and K. P. Roche, Oscillations in exchange coupling and magnetoresistance in metallic superlattice structures: Co/Ru, Co/Cr, and Fe/Cr, Phys. Rev. Lett. **64**, 2304 (1990).
[52] S. S. P. Parkin, R. Bhadra, and K. P. Roche, Oscillatory magnetic exchange coupling through thin copper layers, Phys. Rev. Lett. **66**, 2152 (1991).
[53] S. Liang, R. Chen, Q. Cui, Y. Zhou, F. Pan, H. Yang, and C. Song, Ruderman–Kittel–Kasuya–Yosida-type interlayer Dzyaloshinskii–Moriya interaction in synthetic magnets, Nano Lett. **23**, 8690 (2023).
[54] J. Zou, S. Zhang, and Y. Tserkovnyak, Bell-state generation for spin qubits via dissipative coupling, Phys. Rev. B **106**, L180406 (2022).
[55] B. Heinrich, Y. Tserkovnyak, G. Woltersdorf, A. Brataas, R. Urban, and G. E. W. Bauer, Dynamic exchange coupling in magnetic bilayers, Phys. Rev. Lett. **90**, 187601 (2003).
[56] M. M. Subedi, K. Deng, Y. Xiong, J. Mongeon, M. T. Hossain, P. Meisenheimer, E. Zhou, J. Heron, M. B. Jungfleisch, W. Zhang *et al.*, Magnon-magnon interactions induced by spin pumping-driven symmetry breaking in synthetic antiferromagnets, arXiv:2301.07311.
[57] M. Harder, Y. Yang, B. M. Yao, C. H. Yu, J. W. Rao, Y. S. Gui, R. L. Stamps, and C.-M. Hu, Level attraction due to dissipative magnon-photon coupling, Phys. Rev. Lett. **121**, 137203 (2018).
[58] Y.-P. Wang, J. W. Rao, Y. Yang, P.-C. Xu, Y. S. Gui, B. M. Yao, J. Q. You, and C.-M. Hu, Nonreciprocity and unidirectional invisibility in cavity magnonics, Phys. Rev. Lett. **123**, 127202 (2019).
[59] P.-C. Xu, J. W. Rao, Y. S. Gui, X. Jin, and C.-M. Hu, Cavity-mediated dissipative coupling of distant magnetic moments: Theory and experiment, Phys. Rev. B **100**, 094415 (2019).
[60] Y.-X. Wang, C. Wang, and A. A. Clerk, Quantum nonreciprocal interactions via dissipative gauge symmetry, PRX Quantum **4**, 010306 (2023).
[61] A. Metelmann and A. A. Clerk, Nonreciprocal quantum interactions and devices via autonomous feedforward, Phys. Rev. A **95**, 013837 (2017).
[62] A. J. Daley, Quantum trajectories and open many-body quantum systems, Adv. Phys. **63**, 77 (2014).
[63] G. Srivastava, Phonon conductivity of insulators and semiconductors, J. Phys. Chem. Solids **41**, 357 (1980).
[64] For certain high-quality materials, the lifetime can reach submicrosecond values, leading to the formation of a clear hybrid mode (magnetoelastic mode) that allows information exchange between the magnon and phonon modes. This breakdown of the Markov approximation can be addressed by reducing the phonon lifetime through doping and introducing impurities.
[65] The magnon-environment coupling occurs within a narrow frequency range, approximately the frequency of spacer-induced magnon dynamics (megahertz), where the coupling strength exhibits small variation and can be approximated as constant.
[66] C. W. Gardiner and M. J. Collett, Input and output in damped quantum systems: Quantum stochastic differential equations and the master equation, Phys. Rev. A **31**, 3761 (1985).
[67] A. A. Clerk, M. H. Devoret, S. M. Girvin, F. Marquardt, and R. J. Schoelkopf, Introduction to quantum noise, measurement, and amplification, Rev. Mod. Phys. **82**, 1155 (2010).
[68] A. Clerk, Introduction to quantum non-reciprocal interactions: From non-Hermitian Hamiltonians to quantum master equations and quantum feedforward schemes, SciPost Phys. Lect. Notes 044 (2022).
[69] Y. Zhang, J. Liu, Y. Dong, S. Wu, J. Zhang, J. Wang, J. Lu, A. Rückriegel, H. Wang, R. Duine, H. Yu, Z. Luo, K. Shen, and J. Zhang, Strain-driven Dzyaloshinskii-Moriya interaction for room-temperature magnetic skyrmions, Phys. Rev. Lett. **127**, 117204 (2021).
[70] Y. Liu, X. Huo, S. Xuan, and H. Yan, Manipulating movement of skyrmion by strain gradient in a nanotrack, J. Magn. Magn. Mater. **492**, 165659 (2019).
[71] D. Du, J. Hu, and J. K. Kawasaki, Strain and strain gradient engineering in membranes of quantum materials, Appl. Phys. Lett. **122**, 170501 (2023).
[72] T. Srivastava, M. Schott, R. Juge, V. Krizakova, M. Belmeguenai, Y. Roussigné, A. Bernand-Mantel, L. Ranno, S. Pizzini, S.-M. Chérif *et al.*, Large-voltage tuning of Dzyaloshinskii–Moriya interactions: A route toward dynamic control of skyrmion chirality, Nano Lett. **18**, 4871 (2018).
[73] C.-E. Fillion, J. Fischer, R. Kumar, A. Fassatoui, S. Pizzini, L. Ranno, D. Ourdani, M. Belmeguenai, Y. Roussigné, S.-M. Chérif *et al.*, Gate-controlled skyrmion and domain wall chirality, Nat. Commun. **13**, 5257 (2022).
[74] T. Koyama, Y. Nakatani, J. Ieda, and D. Chiba, Electric field control of magnetic domain wall motion via modulation of the Dzyaloshinskii-Moriya interaction, Sci. Adv. **4**, eaav0265 (2018).
[75] E. Y. Vedmedenko, P. Riego, J. A. Arregi, and A. Berger, Interlayer Dzyaloshinskii-Moriya interactions, Phys. Rev. Lett. **122**, 257202 (2019).
[76] F. Kammerbauer, W.-Y. Choi, F. Freimuth, K. Lee, R. Frömter, D.-S. Han, R. Lavrijsen, H. J. Swagten, Y. Mokrousov, and M. Kläui, Controlling the interlayer Dzyaloshinskii–Moriya interaction by electrical currents, Nano Lett. **23**, 7070 (2023).
[77] M. A. Schoen, D. Thonig, M. L. Schneider, T. Silva, H. T. Nembach, O. Eriksson, O. Karis, and J. M. Shaw, Ultra-low magnetic damping of a metallic ferromagnet, Nat. Phys. **12**, 839 (2016).
[78] J. C. Slonczewski, Current-driven excitation of magnetic multilayers, J. Magn. Magn. Mater. **159**, L1 (1996).
[79] L. Berger, Emission of spin waves by a magnetic multilayer traversed by a current, Phys. Rev. B **54**, 9353 (1996).
[80] G. E. Bauer, E. Saitoh, and B. J. Van Wees, Spin caloritronics, Nat. Mater. **11**, 391 (2012).

[81] O. Chelpanova, A. Lerose, S. Zhang, I. Carusotto, Y. Tserkovnyak, and J. Marino, Intertwining of lasing and superradiance under spintronic pumping, Phys. Rev. B **108**, 104302 (2023).

[82] We can write down the Hamiltonian for this ring structure according to Hamiltonian (5). Note that we assume $G$ to be real and replace $\gamma$ with $2\gamma$ since each magnetic layer is adjacent to two spacer layers.

[83] The function $h(z)$ is obtained by replacing $e^{\pm ik}$ with $z^{\pm 1}$ in $h(k)$.

[84] W.-T. Xue, M.-R. Li, Y.-M. Hu, F. Song, and Z. Wang, Simple formulas of directional amplification from non-Bloch band theory, Phys. Rev. B **103**, L241408 (2021).

[85] C. C. Wanjura, M. Brunelli, and A. Nunnenkamp, Topological framework for directional amplification in driven-dissipative cavity arrays, Nat. Commun. **11**, 3149 (2020).

[86] M. Brunelli, C. C. Wanjura, and A. Nunnenkamp, Restoration of the non-Hermitian bulk-boundary correspondence via topological amplification, SciPost Phys. **15**, 173 (2023).